

## Optical constants of ZnSe in the far infrared

A. Deneuveille\*

*Department of Material Sciences and Engineering, University of Florida, Gainesville, Florida 32611*

D. Tanner

*Department of Physics, University of Florida, Gainesville, Florida 32611*

P. H. Holloway

*Department of Material Sciences and Engineering, University of Florida, Gainesville, Florida 32611*

(Received 6 August 1990)

The absorption coefficient  $\alpha$  and refractive index  $n$  of bulk polycrystalline ZnSe have been derived from transmission measurements over wave-number ranges of 30–200  $\text{cm}^{-1}$  and 250–600  $\text{cm}^{-1}$ . Infrared multiphonon structures have been found and assigned. Variations of  $\alpha$  and  $n$  are satisfactorily described by a single-harmonic-oscillator model for the dielectric constant. Variations in  $\alpha$  caused by multiphonon processes suggest that anharmonic lattice dynamics are important above 250  $\text{cm}^{-1}$ , especially for three-phonon processes, which include the fundamental  $\text{TO}(\Gamma)$  mode.

### INTRODUCTION

ZnSe is a very interesting material for both ultraviolet (uv) and infrared (ir) applications. Near the uv range, its direct band gap of 2.7 eV is well suited for blue-emitting devices to be used in high-definition, full-color displays or for optical storage. In the ir range, ZnSe's low-absorption coefficient outside its narrow reststrahlen band makes it suitable for optical windows. However, there are few reports on its optical constants.

In the ir range, Aven, Marple, and Segall<sup>1</sup> reported the variations of ZnSe's absorption coefficient  $\alpha$  over the wave-number range of  $140 < W < 620 \text{ cm}^{-1}$  from transmission and reflection experiments. Later, Miles<sup>2</sup> focusing on multiphonon absorption reported  $\alpha$  variations in the  $300 < W < 850 \text{ cm}^{-1}$  range from laser calorimetry experiments. However, over the common wave-number range, the absorption values quoted by these two reports disagree by up to an order of magnitude.

The situation is still worse for the reflective index; there is only a brief report of  $n$  and  $k$  variations in the range  $130 < W < 350 \text{ cm}^{-1}$  by Hadni, Claudel, and Strimer<sup>3</sup> from reflection measurements of sintered ZnSe powder. Limited data for refractive index versus wave numbers have been published as internal reports over the range of 1000–10 000  $\text{cm}^{-1}$  (Ref. 4) and 600–10 000  $\text{cm}^{-1}$ .<sup>5</sup>

In this study, both the absorption coefficient  $\alpha$  and the refractive index  $n$  of bulk polycrystalline ZnSe have been measured over the  $W$  ranges of 30–200 and 250–600  $\text{cm}^{-1}$ .

The variations of  $\alpha$  with  $W$  will be compared with the previous contradictory results,<sup>1,2</sup> and peaks due to multiphonon generation will be discussed. Variations of  $n$  with  $W$  will be compared with published data<sup>3</sup> and internal reports.<sup>4,5</sup> Finally, variations of the absorption coefficient and refractive index versus wave numbers will

be compared with a single-harmonic-oscillator model of the fundamental  $\text{TO}(\Gamma)$  lattice mode vibration to predict the dielectric constant of ZnSe.

### EXPERIMENTAL SETUP

The measurements were taken from CVD, Inc. ZnSe polycrystalline discs, 3 and 1.25 mm thick. The average grain size was around 70  $\mu\text{m}$ . The samples were ground, lapped, and polished to a 0.05- $\mu\text{m}$  alumina finish. Some samples were also wedged to decrease the effects of the interference fringes. Samples with thicknesses of 3020, 1240, 424, 350, 118, 91, 45.6, and 22.7  $\mu\text{m}$  were measured. Thicknesses were measured with a micrometer above 100  $\mu\text{m}$ . Below 150  $\mu\text{m}$ , they were deduced from interference fringes in the 30–80  $\text{cm}^{-1}$  range, where the refractive index (calculated from the interference fringes of the thicker samples) has very small variations with the wave numbers. The agreement was good for the sample measured by both methods, 122 and 118  $\mu\text{m}$  using a micrometer and an optical measurement, respectively.

The  $\alpha$  values reported here are extracted only from transmission measurements. Some reflection measurements were also made. They appear much more difficult and less reliable from sample to sample, and so were used here as side measurements. The maximum value of the reflection was found to be  $(89 \pm 2)\%$ , in agreement with previous reports.<sup>1–3</sup>

The optical measurements were done at room temperature with a Fourier-transform infrared spectrometer Brucker IFS 113v with a resolution of 1  $\text{cm}^{-1}$ , using mainly a DTGS detector. Values of  $\alpha$  were calculated from experimental data using intervals of 4  $\text{cm}^{-1}$ .

### RESULTS AND INTERPRETATION

Transmission data for the 3020-, 1240-, 424-, and 91- $\mu\text{m}$ -thick samples (undetected or weak interference

fringes) are given in Fig. 1. The thicker samples show at once that there is a low-absorption coefficient between  $30 < W < 100 \text{ cm}^{-1}$  and  $500 < W < 600 \text{ cm}^{-1}$ . Outside the reststrahlen range  $200 < W < 250 \text{ cm}^{-1}$ , absorption bands appear around 60, 70, 139, 269, 291, 365–68, 413, 435, and  $575 \text{ cm}^{-1}$ . Actually, there is a small dispersion (0.015) in the transmission around  $600 \text{ cm}^{-1}$  when the sample-sample thickness is  $< 150 \mu\text{m}$ . We tentatively attribute it to side effects from the polycrystalline nature of the samples (grain boundaries, etc.). Data from the thickest samples were used to calculate both  $\alpha$  and  $n$  in this wave-number range.

Examples of transmission data with large interference fringes for a 350- and a 118- $\mu\text{m}$ -thick sample over the  $W$  range of 30–200 and 250–600  $\text{cm}^{-1}$ , respectively, are given in Fig. 2. These data were used to derive the refractive index of the material. The same absorption peaks shown in Fig. 1 are observed for these samples.

The transmission (from a "flux" calculation) of a "thick" sample (without interferences fringes or after their removal) is given by<sup>6</sup>

$$T = \frac{(1 - R_i)^2 \exp(-\alpha d)}{1 - R_i^2 \exp(-2\alpha d)}, \quad (1)$$

where the reflectivity  $R_i$  of the air-ZnSe interface is given by

$$R_i = \frac{(n - 1)^2 + k^2}{(n + 1)^2 + k^2}, \quad (2)$$

where  $n$  and  $k$  are the real and imaginary part of the re-

fractive index of ZnSe. In fact, the experimental results were used to calculate  $\alpha$  either in the highly absorbing  $W$  ranges, where  $\exp(-2\alpha d) \leq 5 \times 10^{-2}$ , so that the denominator of Eq. (1) is nearly unity, or for the thickest samples when  $R_i$  is close to 0.25 and 0.2 (Ref. 7) (near 30 and 600  $\text{cm}^{-1}$ , respectively), so that  $1 - R_i^2 \exp(-2\alpha d)$  in Eq. (1) is again approximately unity. As a result,  $T$  can be approximated by

$$T = (1 - R_i)^2 \exp(-\alpha d),$$

for example,

$$\frac{T_1}{T_2} = \exp[-\alpha(d_1 - d_2)].$$

With the sample thicknesses available, this method cannot measure  $\alpha$  values higher than  $10^3 \text{ cm}^{-1}$ . These occur in the range  $200 < W < 250 \text{ cm}^{-1}$ . To minimize any systematic error due to the polycrystalline nature of the samples, the ratios were always calculated between the nearest thicknesses (e.g., 3020/1240, 1240/420, etc.). For the same  $W$  value, the  $\alpha$  values were deduced from several ratios to give an idea of the experimental uncertainty. Values of  $\alpha$  over the ranges of 30–200 and 250–600  $\text{cm}^{-1}$  are shown in Figs. 3 and 4, respectively, for different thickness ratios; the agreement is very good. Values of  $\alpha$  in the range 1–100  $\text{cm}^{-1}$  are observed between 30 and 150  $\text{cm}^{-1}$ .

Values of  $n$  were extracted from the wave-number positions of the interference fringes. The wavelengths  $\lambda$  of the maximum or the minimum are given by the classical

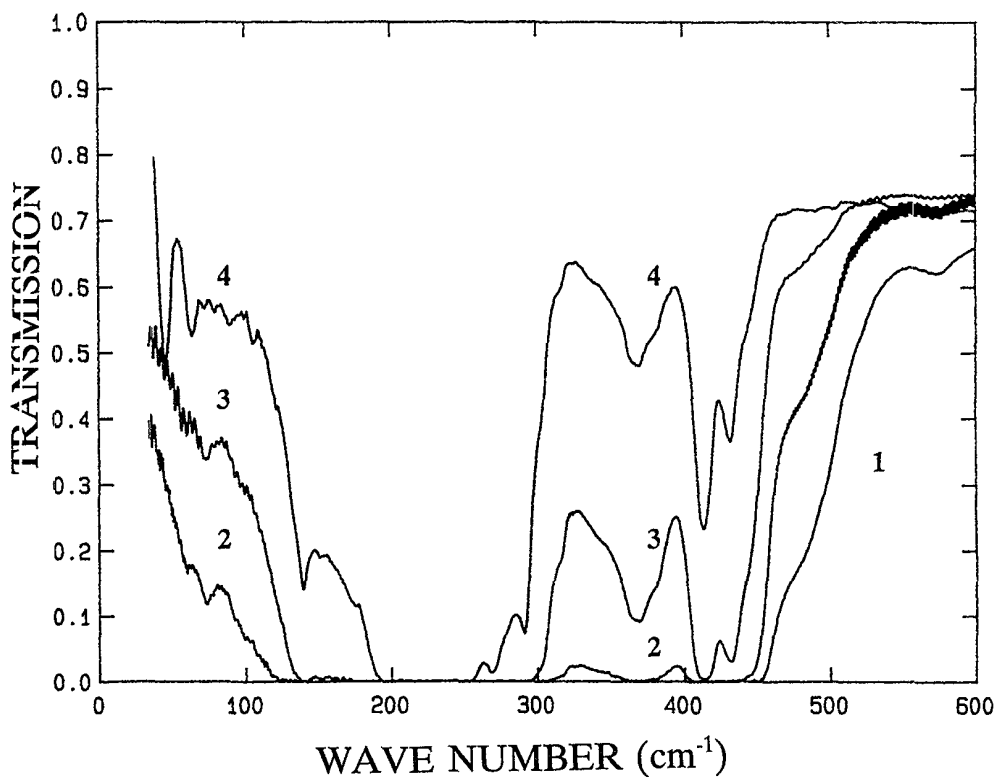


FIG. 1. Transmission vs wave number of some ZnSe samples with undetectable or small interferences fringes. Thickness of sample 1, 400–600  $\text{cm}^{-1}$ , 3020  $\mu\text{m}$ ; sample 2, 30–600  $\text{cm}^{-1}$ , 1240  $\mu\text{m}$ ; sample 3, 30–600  $\text{cm}^{-1}$ , 424  $\mu\text{m}$ ; sample 4, 30–600  $\text{cm}^{-1}$ , 91  $\mu\text{m}$ .

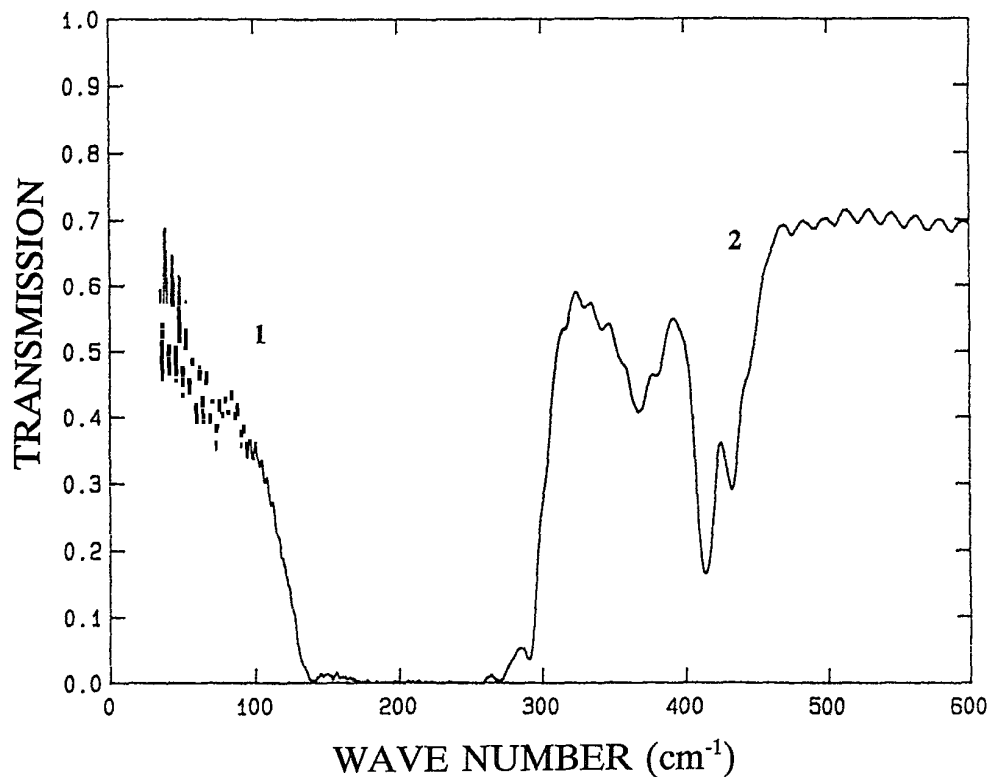


FIG. 2. A composite example of transmission vs wave number of samples with large interference fringes. Sample 1, 0–200  $\text{cm}^{-1}$ , 350  $\mu\text{m}$  thick; sample 2, 250–600  $\text{cm}^{-1}$ , 118  $\mu\text{m}$  thick).

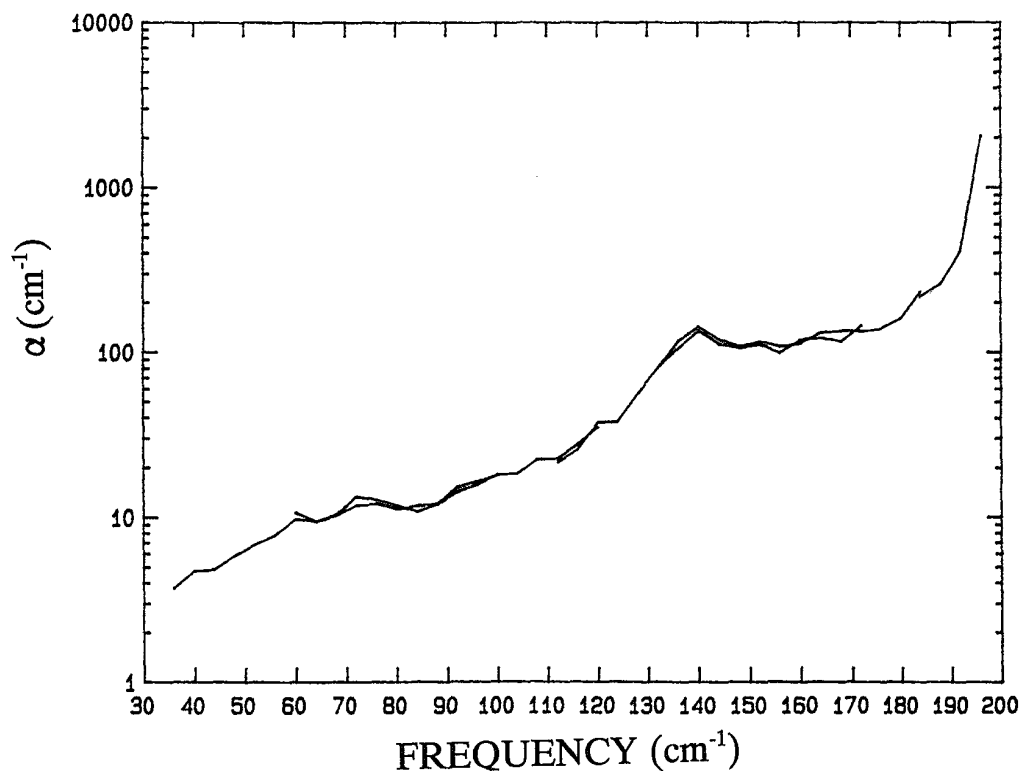


FIG. 3. Variation of the absorption coefficient  $\alpha$  vs wave number  $W$  of ZnSe in the range 30–200  $\text{cm}^{-1}$ .

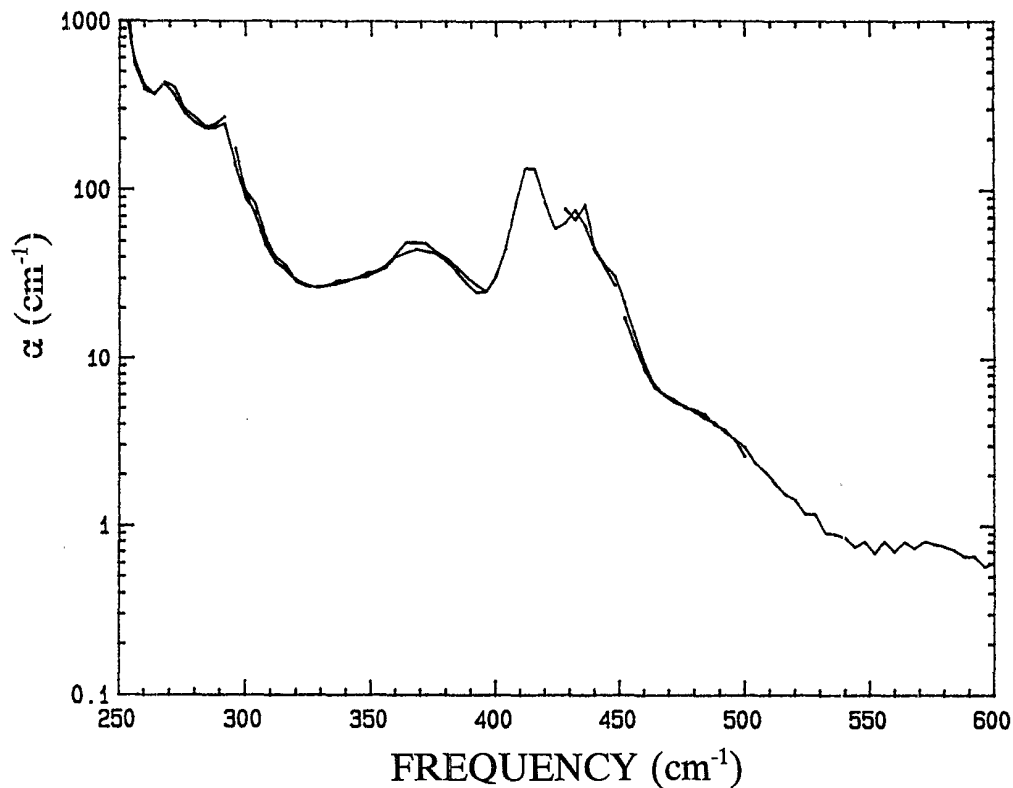


FIG. 4. Variation of the absorption coefficient  $\alpha$  vs wave number  $W$  of ZnSe in the range 250–600  $\text{cm}^{-1}$ .

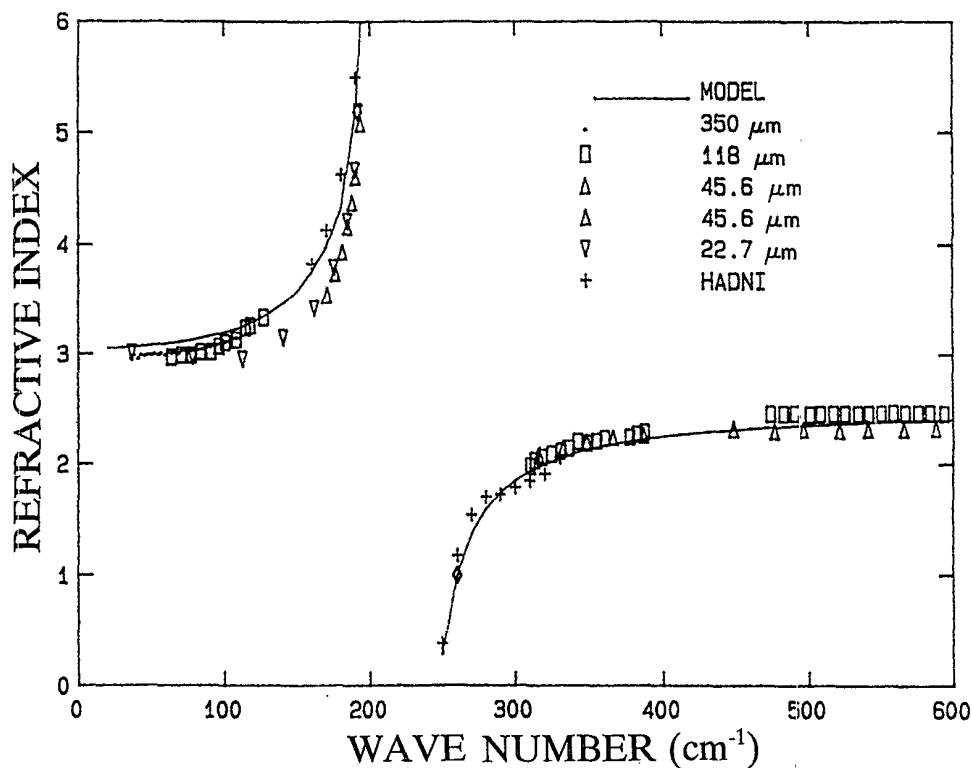


FIG. 5. Variation of the refractive index  $n$  with the wave number  $W$  of ZnSe in the range 30–600  $\text{cm}^{-1}$ ,  $\diamond$  from the position of the minimum in the reflection.

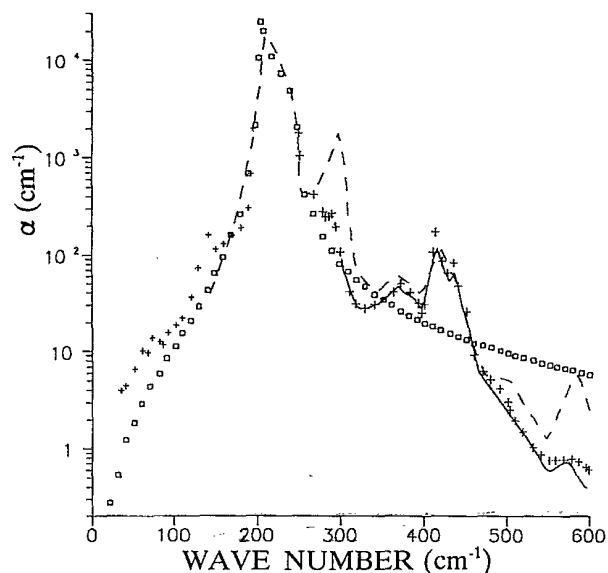


FIG. 6. Comparison of our experimental values (+) of  $\alpha$  vs wave number with the results from Refs. 1 (dashed line) and 2 (solid line), and with the single-harmonic-oscillator model for the dielectric constant ( $\square$ ).

relation

$$2nd = m\lambda/2 = m/2W,$$

where  $m$  is the order of interference.

For the same  $W$ , several  $n$  values were always deduced

from samples of different thicknesses to assess the experimental uncertainty. Values of  $n$  versus wave number are given in Fig. 5. Reasonable agreement is observed between values deduced from samples of different thicknesses. The wave number where  $n=1$ , which corresponds to the minimum of the reflectivity, has been extracted from reflectivity data which are not shown here.

## DISCUSSION

The current variation of  $\alpha$  with wave numbers can be compared to previous results from Aven, Marple, and Segall<sup>1</sup> and Miles<sup>2</sup> (see Fig. 6).

In the common  $W$  range 300–600  $\text{cm}^{-1}$  our results are identical to those of Miles obtained from single crystals by the quite different technique of laser calorimetry.<sup>2</sup> Compared to the results of Aven, Marple, and Segall<sup>1</sup> in the 250–600  $\text{cm}^{-1}$  range, our  $\alpha$  values agree only in the 400–450  $\text{cm}^{-1}$  range and are lower by up to a factor of 10 near 300 and 600  $\text{cm}^{-1}$ . In the 150–200  $\text{cm}^{-1}$  range, the differences are smaller, but they did not report the absorption peak we observed at 139  $\text{cm}^{-1}$  and they have higher  $\alpha$  near 190  $\text{cm}^{-1}$ .

The positions of the absorption peaks are more easily seen from the transmission data in Fig. 1 than from the  $\alpha$  variations in Figs. 3–5. Their  $W$ 's are given in Table I and compared with those found by infrared absorption by Aven, Marple, and Segall,<sup>1</sup> Miles,<sup>2</sup> and Hadni, Claudel, and Strimer<sup>3</sup> or by Raman spectroscopy by Irwin and LaCombe.<sup>8</sup>

TABLE I. Assignments for multiphonon peaks ( $\text{cm}^{-1}$ ) compared with the results of the literature on infrared absorption (Refs. 1–3) and Raman spectroscopy (Ref. 8).

Ref. 1	Ref. 2	Ref. 3 <sup>a</sup>	Ref. 8	This work	Calculated	$\Delta^b$
			38			
			LO-LA(X)			
			50			
			LO-LA(L)			
				60		
				$W_1 - W'_2$	57	+3
				70		
				$W''_2 - W_1$	64	+6
		140	140	139		
		2(TA(X))	2TA(X)	2TA(X)	140	-1
			269	269		
			TO+TA(L)	TO+TA(L)	264	+5
			288	292		
			LO+TA(X)	LO+TA(X)	293	-1
365	365	373	365	365		
		LO+LA	2LA(L)	2LA(L)	362	+3
420	415		412	415		
			2TO	2TO	412	+3
			LO+LA(X)	LO+LA(X)	413	+2
	435	434	430	435		
		LO+TO	LO+TO(X,L)	LO+TO(X,L)	430	+5
585	575			575		
	TO( $\Gamma$ )+2LA(L)			TO( $\Gamma$ )+2LA(L)	568	+7

<sup>a</sup>Data from sintered powder.

<sup>b</sup>Present experiment minus calculated position.

TABLE II. The phonon wave numbers at the main symmetry points of the Brillouin zone from Ref. 8.

TO( $\Gamma$ )	206	TO(X) 206	TO(L) 206
LO( $\Gamma$ )	253	LO(X) 223	LO(L) 224
		TA(X) 70	TA(L) 58
		LA(X) 190	LA(L) 181
$W_3$	201		
$W_1$	150		
$W_2'$	93		
$W_2''$	214		
$W_4'$	115		
$W_4''$	213		

The agreement in peak positions is good for all authors above 300  $\text{cm}^{-1}$ . Below 300  $\text{cm}^{-1}$ , we found peaks at 292, 269, and 159  $\text{cm}^{-1}$  in agreement with data from Irwin and LaCombe from Raman spectroscopy. Peaks at 60 and 70  $\text{cm}^{-1}$  were not previously reported, and peaks at 116, 50, and 38  $\text{cm}^{-1}$  reported by these authors were not observed.

The origin of structure outside the reststrahlen range (200–250  $\text{cm}^{-1}$ ) is currently assigned to multiphonon excitation either from direct excitation of higher moments in the polarization<sup>9</sup> or by indirect excitation by the TO( $\Gamma$ ) mode through anharmonic lattice dynamics.<sup>10–13</sup> In both case, the peak positions must be linear combinations of the wave number of the optical and acoustical phonons, mainly at the edges or at the center of the Brillouin zone. The wave numbers corresponding to the phonons at the main symmetry points of ZnSe are already quoted in the literature, mainly from Raman spectroscopy. The most recent values of Irwin and LaCombe<sup>8</sup> (which are in close agreement with those deduced independently by Hennion *et al.*<sup>14</sup> from neutron diffraction) are given in Table II.

Our assignments of the lines are compared with those of previous authors in Table I. Also shown are peak positions calculated from our assignments and the phonon wave numbers of Table II, along with the difference  $\Delta$  between the experimental and calculated values. There is good agreement between our experimental and calculated values for all lines, the worse agreement being +7  $\text{cm}^{-1}$  [TO( $\Gamma$ )+2LA(L) at 575  $\text{cm}^{-1}$ ], +6  $\text{cm}^{-1}$  ( $W_2'' - W_1$  at 70  $\text{cm}^{-1}$ ), and +5  $\text{cm}^{-1}$  [TO(L)+TA(L) at 269  $\text{cm}^{-1}$  and LO(X,L)+TO(X,L) at 430  $\text{cm}^{-1}$ ]. Notice that only the 575- $\text{cm}^{-1}$  peak involves a combination with the fundamental TO( $\Gamma$ ) lattice vibration mode.

The values of  $\alpha$  and  $n$  may be compared with the simplest single-harmonic-oscillator model for the ZnSe dielectric constant,<sup>3,15</sup> where the complex dielectric constant  $K$  is given by

$$K = K_\infty + \frac{W_{\text{TO}}^2(K_0 - K_\infty)}{W_{\text{TO}}^2 W^2 + i\gamma_p W}$$

with  $K = K_1 - iK_2$ .

In this model, the values of  $K_1$ ,  $K_2$ ,  $n$ ,  $k$ , and  $a$  are given by<sup>15</sup>

$$K_1 = K_\infty + \frac{W_{\text{TO}}^2(K_0 - K_\infty)(W_{\text{TO}}^2 - W^2)}{(W_{\text{TO}}^2 - W^2)^2 + \gamma_p^2 W^2},$$

$$K_2 = \frac{W_{\text{TO}}^2(K_0 - K_\infty)\gamma_p W}{(W_{\text{TO}}^2 - W^2)^2 + \gamma_p^2 W^2},$$

$$n = \frac{[(K_1^2 + K_2^2)^{1/2} + K_1]^{1/2}}{2^{1/2}},$$

$$k = \frac{[(K_1^2 + K_2^2)^{1/2} - K_1]^{1/2}}{2^{1/2}},$$

and  $\alpha = 4\pi k W$ .

To evaluate this model the wave number  $W_{\text{TO}}$  of the TO phonon mode in the center ( $\Gamma$ ) of the Brillouin zone along with its damping coefficient  $\gamma_p$  and the dc  $K_0$  and optical  $K_\infty$  dielectric constant for ZnSe are needed. The values used in the present study are compared in Table III with those reported previously by Riccius<sup>16</sup> and Hadni, Claudel, and Strimer<sup>3</sup> to fit their reflectivity data. The absorption coefficient  $\alpha$  and the reflectivity values in the (maximum) range 200–250  $\text{cm}^{-1}$ , are very sensitive to  $\gamma_p$ . Lower- $\gamma_p$  values would correspond to higher  $\alpha$  near its maximum but lower- $\alpha$  values at lower and higher wave numbers, which would have given slightly better direct agreement between the model and our experimental points. However, in order to agree with the reflectivity data and the maximum  $\alpha$  value of Aven, Marple, and Segall<sup>1</sup> the optimum  $\gamma_p$  has to be close to the previously quoted values. The experimental absorption curve (involving multiphonon components) is compared to the calculated curve [taking only into account the fundamental lattice vibration mode TO( $\Gamma$ ) with an energy-independent damping coefficient; "harmonic model"] in Fig. 6. Below 200  $\text{cm}^{-1}$ , the agreement between the experimental curves and the model is good. There is no clear trend for the origin of the multiphonon excitation. Between 250 and 450  $\text{cm}^{-1}$ , the comparison shows that with the usual value of  $\gamma_p = 4.53 \text{ cm}^{-1}$ , the structures assigned to two phonons generally lie at  $\alpha$ 's above those predicted by the model, while the minimum in between are slightly below the model prediction. This suggests a significant anharmonic lattice contribution, which would introduce an additional wave-number-dependent damping for the TO( $\Gamma$ ) mode from the two-phonon excitations. Above 450  $\text{cm}^{-1}$ , where the three-phonon structures are assigned to a coupling of the TO( $\Gamma$ ) fundamental mode with two phonons at the edge of the Brillouin zone,<sup>2</sup> experimental  $\alpha$ 's are always lower than those of the model. This suggests a dominance of anharmonic lattice dynamics, which introduces a large additional damping of the TO( $\Gamma$ ) mode. The trend towards the dominance of anharmonicity effects when going to higher-multiphonon processes is quite general,<sup>10–13</sup> but it is especially obvious here, where three phonons, including TO( $\Gamma$ ), are involved.

Variation of the refractive index  $n$  with  $W$  are compared with previous values from the literature in Fig. 5. In the lower- $W$  range (30–120  $\text{cm}^{-1}$ ),  $n$  values derived from the positions of the interference fringes of the 350- and 118- $\mu\text{m}$ -thick samples are in close agreement. Be-

TABLE III. Our parameters for the calculations of  $\alpha$  and  $n$  from the single-harmonic-oscillator model, compared to those of the literature (Refs. 3 and 16).

	$W_{\text{TO}}$	$K_0$	$K_\infty$	$\gamma_p$
Ref. 3	204.2	9.3	6.2	4.49
Ref. 16	209.5	9.2	6.2	4.60
This work	206	9.3	6.2	4.53

tween 150 and 195  $\text{cm}^{-1}$ ,  $n$  values deduced from the interference fringes of the thinner samples, 45.6 and 22.7  $\mu\text{m}$  thick, are also very close. Finally, values above 300  $\text{cm}^{-1}$  are deduced from the 118- and 45.6- $\mu\text{m}$ -thick samples and are also in good agreement.

Below and above the reststrahlen, our values of  $n$  are slightly lower and higher, respectively, than those of Hadni, Claudel, and Strimer.<sup>3</sup> They agree with those reported by the manufacturer (CVD, Inc.) around 600  $\text{cm}^{-1}$  and around 30  $\text{cm}^{-1}$  with the dc dielectric constant quoted by the literature.<sup>7</sup>

Our experimental values are in good agreement with those of the model (see parameters in Table III), being slightly lower and very close below and above the reststrahlen region, respectively.

Finally, our results on bulk polycrystalline ZnSe are in good agreement with those for  $\alpha$  on bulk monocrystalline ZnSe and even with those for  $n$  from sintered ZnSe powder. This indicates a dominance of the local structure on the ir properties of ZnSe.

### CONCLUSION

The refractive index  $n$  and the absorption coefficient  $\alpha$  of bulk polycrystalline ZnSe have been measured over the wave-number ranges of 30–200 and 250–600  $\text{cm}^{-1}$ .

The present  $\alpha$  measurements between 30–150  $\text{cm}^{-1}$  are the first reported for ZnSe. Our results are identical

to those of Miles<sup>2</sup> from bulk monocrystalline material over the common range 300–600  $\text{cm}^{-1}$ . They differ significantly from those quoted in the pioneering work of Aven, Marple, and Segall<sup>1</sup> over most of the  $\alpha$  ranges.

Multiphonons effects are clearly seen in the  $\alpha(W)$  data. Most frequencies agree with those reported previously from ir absorption in bulk monocrystalline ZnSe.<sup>1,2</sup> Additional structures previously reported from Raman spectroscopy were also found at 392, 269, and 139  $\text{cm}^{-1}$ . New structures were reported near 60 and 70  $\text{cm}^{-1}$  and have been tentatively assigned to  $W_1 - W'_2$  and  $W'_2 - W_1$  phonon combinations.

The  $\alpha$  values are in reasonable agreement with a harmonic-oscillator model of the dielectric constant for the fundamental lattice vibrations of the  $\text{TO}(\Gamma)$  mode with  $W_{\text{TO}} = 206 \text{ cm}^{-1}$ , a damping coefficient of  $\gamma_p = 4.53 \text{ cm}^{-1}$ ,  $K_0 = 9.3$ , and  $K_\infty = 6.2$ . The absorption coefficient  $\alpha$  is slightly modified by multiphonon effects when  $30 < \alpha < 450 \text{ cm}^{-1}$  (two phonons), and drastically modified above 450  $\text{cm}^{-1}$  (three phonons). Above 250  $\text{cm}^{-1}$ , analysis suggests a significant influence of the lattice anharmonicity beginning with the two-phonon effect, and becoming dominant for three phonons. For three phonons involving the fundamental  $\text{TO}(\Gamma)$  mode, the additional damping is especially important.

The first  $n$  measurements on solid ZnSe in the range 30–600  $\text{cm}^{-1}$  are reported here. They are in reasonable agreement with those of Hadni, Claudel, and Strimer<sup>3</sup> on ZnSe sintered powder over the ranges 130–195 and 250–350  $\text{cm}^{-1}$ . They are also in reasonable agreement with the prediction of a single-oscillator model for the dielectric constant of ZnSe.

### ACKNOWLEDGMENTS

This work was supported by U.S. Defense Advanced Research Projects Agency (DARPA) Grant No. MDA 972-88-J-1006.

\*Permanent address: Laboratoire d'études des propriétés électroniques des solides, Centre National de la Recherche Scientifique, Boîte Postal 166 X, 38042 Grenoble CEDEX, France.

<sup>1</sup>M. Aven, D. T. F. Marple, and B. Segall, *J. Appl. Phys. Suppl.* **32**, 2261 (1961).

<sup>2</sup>P. A. Miles, *Appl. Opt.* **16**, 2891 (1977).

<sup>3</sup>A. Hadni, J. Claudel, and P. Strimer, *Phys. Status Solidi* **26**, 241 (1986).

<sup>4</sup>A. J. Jones, Hughes Aircraft Company Report No. AD 704 555, 1970 (unpublished).

<sup>5</sup>CVD Inc. report (unpublished).

<sup>6</sup>See, for example, H. Y. Fan and M. Becker, in *Proceedings of the Reading Conference on Semiconducting Materials*, edited by H. K. Henish (Butterworth, London, 1951), p. 132.

<sup>7</sup> $R_1$  near 30 and 600  $\text{cm}^{-1}$  can be estimated, *a priori*, from the dc

and optical dielectric constants published in the literature, e.g., H. Ruda, *J. Appl. Phys.* **59**, 1220 (1986).

<sup>8</sup>J. C. Irwin and J. C. Lacombe, *Can. J. Phys.* **50**, 2596 (1972).

<sup>9</sup>B. Bendow, S. P. Yukon, and See-Chen Yin, *Phys. Rev. B* **10**, 2286 (1974).

<sup>10</sup>T. J. McParker, J. R. Birch, and C. L. Mock, *Solid State Commun.* **36**, 581 (1980).

<sup>11</sup>D. L. Mills and A. A. Maradudin, *Phys. Rev. B* **8**, 1617 (1973).

<sup>12</sup>B. Bendow, See-Chen Yin, and S. P. Yukon, *Phys. Rev. B* **8**, 1679 (1973).

<sup>13</sup>M. Sparks and L. J. Sham, *Phys. Rev. B* **8**, 3037 (1973).

<sup>14</sup>B. Hennion, F. Moussa, G. Pepy, and K. Kunck, *Phys. Lett.* **36A**, 376 (1971).

<sup>15</sup>See, for example, J. S. Blakemore, *J. Appl. Phys.* **53**, R123 (1982).

<sup>16</sup>H. D. Riccius, *J. Appl. Phys.* **39**, 4381 (1968).